JOURNAL OF MATERIALS SCIENCE 21 (1986) 4015–4018

High-temperature creep and dislocation structure of MgO single crystals at low stresses

K. S. RAMESH, EIICHI YASUDA, SHIUSHICHI KIMURA
Research Laboratory of Engineering Materials, Tokyo Institute of Technology, 4259 Nagatsuta, Midori-ku, Yokohama 227, Japan

KAZUYORI URABE
Department of Inorganic Materials, Tokyo Institute of Technology, O-okayama, Meguro-ku, Tokyo 153, Japan

MgO single crystals oriented toward (1 0 0) have been compressively deformed to strains in the range of 0.04 to 0.09 at temperatures between 1948 and 2023 K using stresses under 6 MPa. Microstructural developments in the crept samples were monitored by etch pitting, SEM and HVEM. Optical microscopy revealed an equiaxed network of subgrains with ⟨1 1 0⟩ forming the framework for the formation of subgrains. Measurement of the dislocation density not associated with cells reveals that the stress dependence of the steady-state values of dislocation density can be described by the relation $\varrho \propto \sigma^{2.15}$. HVEM observations show that cell boundaries are formed by the process of knitting. Drastic unloading results in a fraction of the sub-boundaries straightening, but the majority of the boundaries are destroyed. It is concluded that creep of MgO at low stresses and high temperature is similar to those of f c c metals.

1. Introduction

The creep behaviour of MgO has been the subject of investigation by several authors [1–4]. These studies have primarily been confined to high stresses. But in actual practice most high-temperature engineering applications are concerned with long-term exposures involving relatively low stresses [5]. In order to provide a better understanding of the creep mechanisms at high temperatures and low stresses, the present study was initiated in an effort to obtain detailed and precise information on dislocation structures that develop during the process of creep on loading and unloading, and to explore the relation to (a) dislocation structure, dislocation density and cell formation, and (b) the stress dependence of dislocation density and cell diameter during steady-state creep.

2. Experimental procedure

The single crystals used in the present study contained 10 p.p.m. (Na + K), 300 p.p.m. Si, 330 p.p.m. Ca, 70 p.p.m. Fe and < 10 p.p.m. (Ti + Ni). The samples were in the form of parallelepipeds normally 4 mm × 4 mm × 8 mm and were chemically polished before testing.

The samples were deformed under compression in a high-precision high-temperature creep equipment. The construction of the equipment is given in detail elsewhere [6]. The majority of the tests were run between 1948 and 2023 K, and the stresses ranged from 6 MPa down to 1.5 MPa. Strain measurements were monitored with a pair of linear variable differential transformers (LVDTs) with an accuracy of better than 10^{-5} cm. To maintain the dislocation structure produced during deformation, samples were cooled at the rate of 10° C min^{-1}.

Microstructural observations were performed in sections along the (0 0 1) plane parallel to the stress axis. These sections were chemically polished in 85% phosphoric acid at 140° C. After X-ray examination with a Laue back-reflection camera, they were etched in a 0.35M solution of sulphuric acid for 10 min to reveal the dislocation structure for optical microscopy.

For scanning electron microscopy of (0 0 1), the specimens were decorated with gold before examination while for HVEM the slices were chemically polished down to 1 mm before thinning to a few tens of nanometres. Specimens prepared in this way were examined at 1000 kV.

3. Results and discussions

3.1. Creep observations

With single crystals a steady-state condition was observed to have been reached after creep strain in excess of 0.09, with the strain rate decaying rapidly to an almost constant value after 0.06. The stress dependence of the steady-state creep rate was investigated in the range of 1.5 to 6 MPa between 1948 and 2023 K. In the investigated range, a transition in the stress exponent, n, from 3 at stresses higher than 2 MPa to almost unity at lower stress was observed [6]. The activation area of steady state was calculated after Blum and Reppich [7] and found to be $105\,b^2$, where b is Burgers vector. The magnitude of the activation area compares favourably with the values for metals and NaCl [8].

3.2. Creep structures

3.2.1. X-ray studies

Laue back-reflection X-ray diffraction patterns of a

0022–2461/86 $03.00 + .12

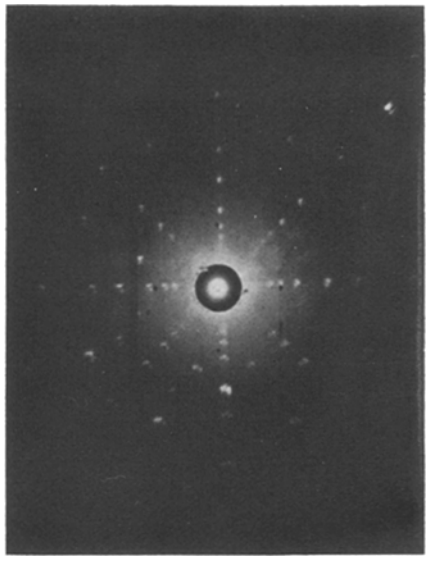

Figure 1 Laue back-reflection X-ray pattern of MgO single crystal crept to a strain of 0.09 at 1973 K under 2 MPa.

(1 1 0) face parallel to the compression axis showed evidence for polygonization after a plastic strain of 0.09, as shown by the breaking up of elongated spots. A typical X-ray pattern is shown in Fig. 1.

3.2.2. Etch pit studies

The microstructure feature involves the generation of a subgrain network (Fig. 2). These subgrains were observed on polished and etched samples. The subgrain formation was observed mostly in samples crept to a strain greater than 0.04 at a temperature of 1948 K. The dislocation structure during primary creep consisted of parallel cell walls. However, the subgrain became equiaxial after a strain of 0.09, contrary to the observations of Huther and Reppich [9] who did not observe a steady state before a strain of 0.4. This dislocation structure is typical for steady state creep [9].

A log–log plot of dislocation density not associated with subgrain cells as a function of stress at 2023 K is shown in Fig. 3. This gives the following relationship:

$$\varrho \propto \sigma^{2.15}$$

A lower stress exponent of 1.4 for steady-state values of dislocation density as a function of stress was observed for MgO by Huther and Reppich [9]. Sinha *et al.* [10] reported the stress dependency of the dislocation velocity for MgO single crystals for temperatures up to 1000 K. The stress exponent extrapolated to 2000 K yields 0.5. The creep rate can be expressed as the product of dislocation velocity, Burgers vector and dislocation density. The stress exponent calculated from the dislocation density and dislocation velocity was found to be 2.8, which agrees well with the measured value of $n = 3$ reported earlier [6].

3.2.3. Scanning electron microscopy

Typical stucture as revealed by SEM is shown in Fig. 4. An interesting feature is the near absence of dislocation inside these cells. This is consistent with the fact that the density of dislocations within subgrains, and therefore the recovery rate, is reduced continuously with increasing creep strain, approaching a constant level at the onset of steady-state creep [11]. Subgrain size was measured on a number of etch pit micrographs by the method of Smith and Guthmann [12]. It was observed that the subgrain diameter decreases with increasing applied stress and is strongly dependent on applied stress (Fig. 5). The variation of subgrain size with dependency for stress can be written as

$$d = K\mu M\boldsymbol{b}/\sigma$$

where d = subgrain size, M = schmid factor, μ = shear modulus, $\boldsymbol{b}$ = Burgers vector and σ = applied stress. The value of K was found to be 9. Relations of the type given in the above equation are commonly found to hold [13]. The product of K and M for MgO was found to be 18. This value compares well with the stress dependence of subgrain size found for ionic crystals and metals by others, for example, 35 in NaCl [14], 28 in AlZn [15] and 40 in LiF [16].

3.3. Effect of stress reduction on structure

Fig. 6 shows the microstructure of MgO single crystal after creep at 1973 K into the steady state, followed by 30 min recovery after partial unloading to 1.98 MPa. The line AB clearly indicates a misorientation due to the presence of a sub-boundary. On the other hand, dislocations in Zones C and D indicate they are mobile and not part of a sub-boundary. The presence of a triple point between C and D demonstrates that by movement of dislocations during the deformation

Figure 2 Evolution of dislocation substructure at different strain levels at 4 MPa and 2023 K. Strain (a) 0.02, (b) 0.04, (c) 0.09.

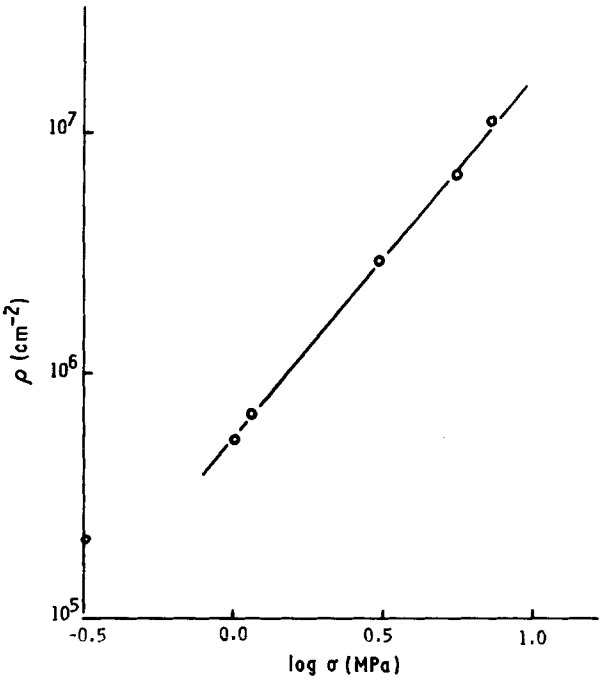

Figure 3 Dislocation density not associated with subgrain cells as a function of applied stress at 2023 K.

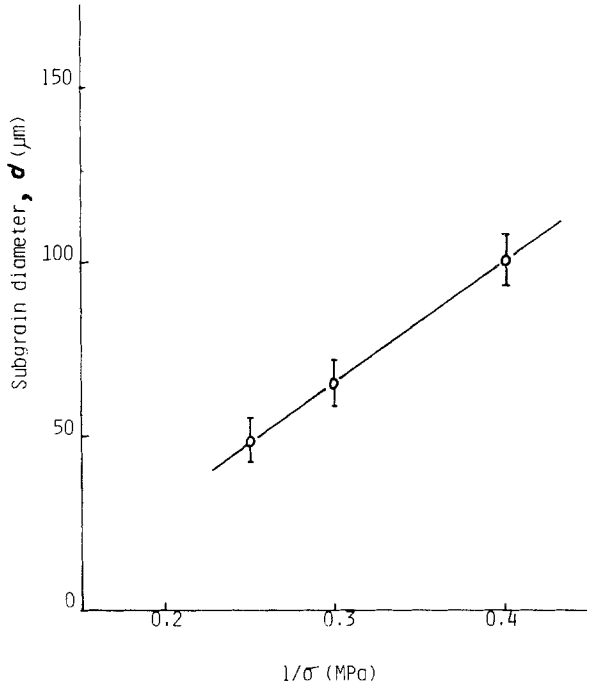

Figure 5 Subgrain diameter as a function of reciprocal of applied stress at 2023 K: $d = K\mu Mb/\sigma$.

process coalescence of grain boundaries was taking place. This amply corroborates the results of Excell and Warrington [17] and Eggeler and Blum [13] that during stress reduction, dissolution of subgrain boundaries and boundary migration take place. During the transient creep large subgrains grow by boundary migration and further sub-division into smaller cells, until the new steady state is closely approached by the larger subgrains. This microstructure shows that boundaries are formed by a knitting phenomenon as proposed for fcc metals by Lindroos and Miekkoja [18, 19].

However, upon complete unloading the majority of sub-boundaries are destroyed (Fig. 7). This is in contradiction with the conclusions of several authors [20–23] who have reported that sub-boundaries cannot be destroyed by means of thermoactivation [23]. It seems that total or partial unloading of stress can lead to a rapid relaxation of structure, and especially of sub-boundaries. The dislocations move in the reverse direction [24]. In this process, a fraction of the sub-boundaries get straightened, but the majority of the boundaries can be destroyed. The effect is stronger, the higher the temperature [25]. Such a behaviour has also been observed in aluminium metal at medium temperatures [23].

The process of cell destruction is still not clear in aluminium metal [26]. What is clear is that local stress concentrations help dislocations to merge into cell walls or to be extracted from them. The two main stress concentrations are irregularities in the lattice of dislocations building the cell walls, but also non-equilibrium conditions at cell edges and cell summits. In the temperature range of this study it can be expected that we are in the climb regime. If this is true, it can be expected that stress concentrations from irregularities in the cell walls will disappear quickly. However, stress concentrations at cell edges and summits would probably remain. Such stress concentrations are a sign of lack of equilibrium (which can be expected to be partly induced by the applied stress and also originate from the kinetics of the growth of the cells); under removal of the applied stresses, such a lack of equilibrium might induce a destruction of the cell structure. There seems to be a qualitative analogy with the Bauschinger effect [26].

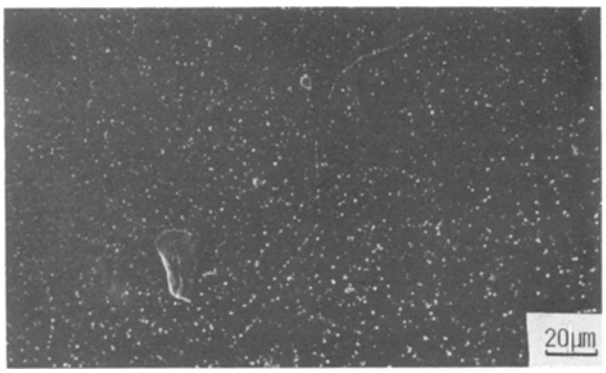

Figure 4 Scanning electron micrograph of sample strained to 0.09 at 4 MPa and 2023 K, showing low density of dislocation etch pits inside subgrain cells.

4. Conclusion

The experimental results demonstrate that creep behaviour, as well as the stress dependence of the dislocation structure developed during creep at high temperature and low stresses, is very similar to that of fcc metals.

Acknowledgements

The authors are grateful to Dr D. Caillard of Laboratoire d'Optique Electronique du CNRS, France and to Professor Brian Wilshire, University College, Swansea, UK for helpful discussions.

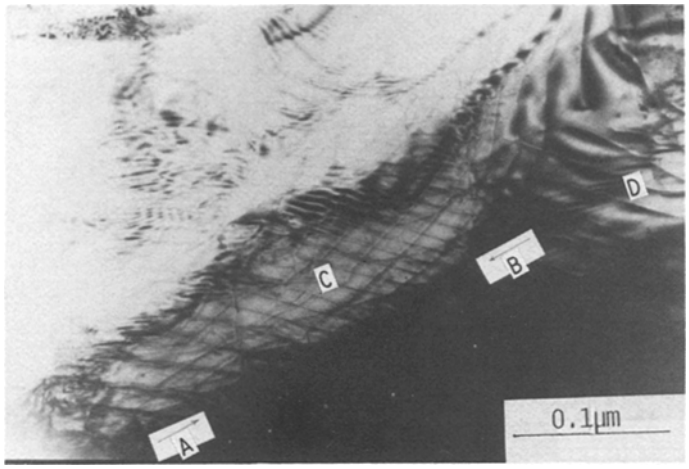

Figure 6 Bright-field HVEM of a sample crept to steady state at 2.5 MPa and 1973 K and followed by 30 min recovery at 1.98 MPa at the same temperature.

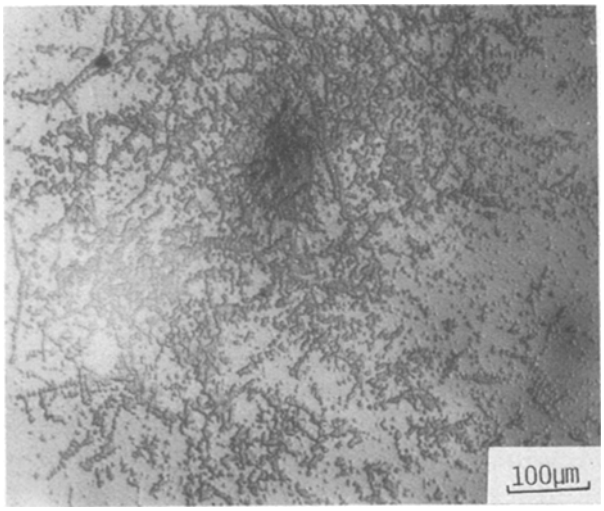

Figure 7 Optical micrograph of MgO strained to 0.09 at 2.5 MPa and 2023 K followed by complete unloading, showing the destruction of substructure.

References

1. C. O. HULSE, S. M. COPLEY and J. A. PASK, *J. Amer. Ceram. Soc.* **46** (1963) 317R.
2. R. B. DAY and R. J. STOKES, *ibid.* **49** (1966) 345.
3. J. B. BILDE-SORENSEN, *ibid.* **55** (1973) 606.
4. J. M. BIRCH and B. WILSHIRE, *J. Mater. Sci.* **9** (1974) 794.
5. B. WILSHIRE, *Proc. Br. Ceram.* No. 32 (1982) 107.
6. E. YASUDA, K. S. RAMESH, S. KIMURA, H. ISHII and M. MUNAKATA, *Yogyo Kyokai shi* **94** (1986) 536.
7. W. BLUM and B. REPPICH, *Acta Metall.* **17** (1969) 959.
8. W. BLUM and B. ILSCHNER, *Phys. Status Solidi* **20** (1967) 629.
9. W. HUTHER and B. REPPICH, *Phil. Mag.* **28** (1973) 363.
10. M. N. SINHA, D. J. LLOYD and T. TANGRI, *ibid.* **28** (1973) 1341.
11. B. SIDEY and B. WILSHIRE, *Met. Sci. J.* **3** (1969) 56.
12. C. S. SMITH and L. GUTTMAN, *Trans. Amer. Inst. Min. Engr.* **197** (1953) 81.
13. G. EGGELER and W. BLUM, *Phil. Mag.* **44** (1981) 1065.
14. J. P. POIRIER, *ibid.* **26** (1972) 713.
15. W. BLUM, A. ABSENGER and F. FEILHAUER, in Proceedings of 5th International Conference on Strength of Metals and Alloys, Aachen, edited by P. Hassen (Pergamon, 1980) p. 265.
16. G. STREB and B. REPPICH, *Phys. Status Solidi (a)* **16** (1973) 493.
17. S. EXCELL and D. WARRINGTON, *Phil. Mag.* **26** (1972) 1121.
18. V. K. LINDROOS and H. M. MIEKKOJA, *ibid.* **16** (1967) 593.
19. *Idem, ibid.* **17** (1968) 119.
20. J. FRIEDEL, "Dislocations" (Pergamon Press, Oxford, 1964).
21. J. P. HIRTH and J. LOTHE, "Theory of dislocations" (McGraw-Hill, New York, 1968).
22. S. AMELINCKX and W. DEKEYSER, *Sol. State Phys.* **8** (1959) 325.
23. M. M. MYSHLYAEV, *Fiz. Tverd. Tela* (in Russian) **12** (1970) 860.
24. K. S. RAMESH, EIICHI YASUDA and SHIUSHICHI KIMURA, *J. Mater. Sci.* **21** (1986) 3147.
25. M. M. MYSHLYAEV, private communication (1985).
26. J. FRIEDEL, private communication (1985).

Received 26 November 1985
and accepted 4 February 1986